Nucleic Acids Research, 2005, Vol. 33, No. 17 ***5677–5690***
doi:10.1093/nar/gki862

Crystal structures of complexes between aminoglycosides and decoding A site oligonucleotides: role of the number of rings and positive charges in the specific binding leading to miscoding

Boris François, Rupert J. M. Russell[1], James B. Murray[1], Fareed Aboul-ela[1], Benoît Masquida, Quentin Vicens and Eric Westhof*

Institut de biologie moléculaire et cellulaire du CNRS, UPR9002 'Architecture et Réactivité de l'ARN', Université Louis Pasteur, F-67084 Strasbourg, France and [1]Vernalis (R&D), Granta Park, Cambridge, CB1 6GB, UK

Received July 24, 2005; Revised and Accepted September 7, 2005

ABSTRACT

The crystal structures of six complexes between aminoglycoside antibiotics (neamine, gentamicin C1A, kanamycin A, ribostamycin, lividomycin A and neomycin B) and oligonucleotides containing the decoding A site of bacterial ribosomes are reported at resolutions between 2.2 and 3.0 Å. Although the number of contacts between the RNA and the aminoglycosides varies between 20 and 31, up to eight direct hydrogen bonds between rings I and II of the neamine moiety are conserved in the observed complexes. The puckered sugar ring I is inserted into the A site helix by stacking against G1491 and forms a pseudo base pair with two H-bonds to the Watson–Crick sites of the universally conserved A1408. This central interaction helps to maintain A1492 and A1493 in a bulged-out conformation. All these structures of the minimal A site RNA complexed to various aminoglycosides display crystal packings with intermolecular contacts between the bulging A1492 and A1493 and the shallow/minor groove of Watson–Crick pairs in a neighbouring helix. In one crystal, one empty A site is observed. In two crystals, two aminoglycosides are bound to the same A site with one bound specifically and the other bound in various ways in the deep/major groove at the edge of the A sites.

INTRODUCTION

Aminoglycosides are broad spectrum bactericidal antibiotics which are used against Gram-negative bacteria such as *Escherichia coli* and some Gram-positive bacteria such as those of the *Staphylococcus* family. They disturb the fidelity of the tRNA selection step during protein synthesis by binding to the A site on the bacterial ribosome 16S rRNA (1,2). The aminoglycoside antibiotics are oligosaccharides containing variable numbers of sugar rings and ammonium groups (3). They all contain a central 2-deoxystreptamine (2-DOS or ring II) with an ammonium group on either side of the deoxy carbon and attached at position 4 to ring I, forming the neamine molecule. The different sub-classes can be distinguished on the basis of the chemical linkages to ring II: in the neomycin family (containing paromomycin, neomycin B, lividomycin A and ribostamycin), ring II is 4,5-disubstituted and, in the kanamycin and gentamicin families (to which tobramycin, geneticin and gentamicin C1A belong), ring II is 4,6-disubstituted (Figure 1).

A critical advance in the understanding of molecular recognition and the mechanisms of action has recently been made with the high-resolution crystal structures (3.1 Å) of bacterial ribosomal 30S particles complexed to aminoglycosides (4–7). In addition, crystal structures were solved for the decoding-aminoacyl site (A site) (2.4–2.54 Å), isolated from the bacterial ribosome 16S rRNA, and complexed with several antibiotics from the aminoglycoside family (8–10). The crystalline complexes between RNA oligonucleotides containing two A sites (Figure 2) and paromomycin, tobramycin or

*To whom correspondence should be addressed. Tel: +33388417046; Fax: +33388601822; Email: e.westhof@ibmc.u-strasbg.fr
Present addresses:
Fareed Aboul-ela, Department of Biological Sciences, Louisiana State University, Baton Rouge, LA 70803, USA
Quentin Vicens, Department of Chemistry and Biochemistry, Howard Hughes Medical Institute, University of Colorado, Boulder, CO 80309-0215, USA

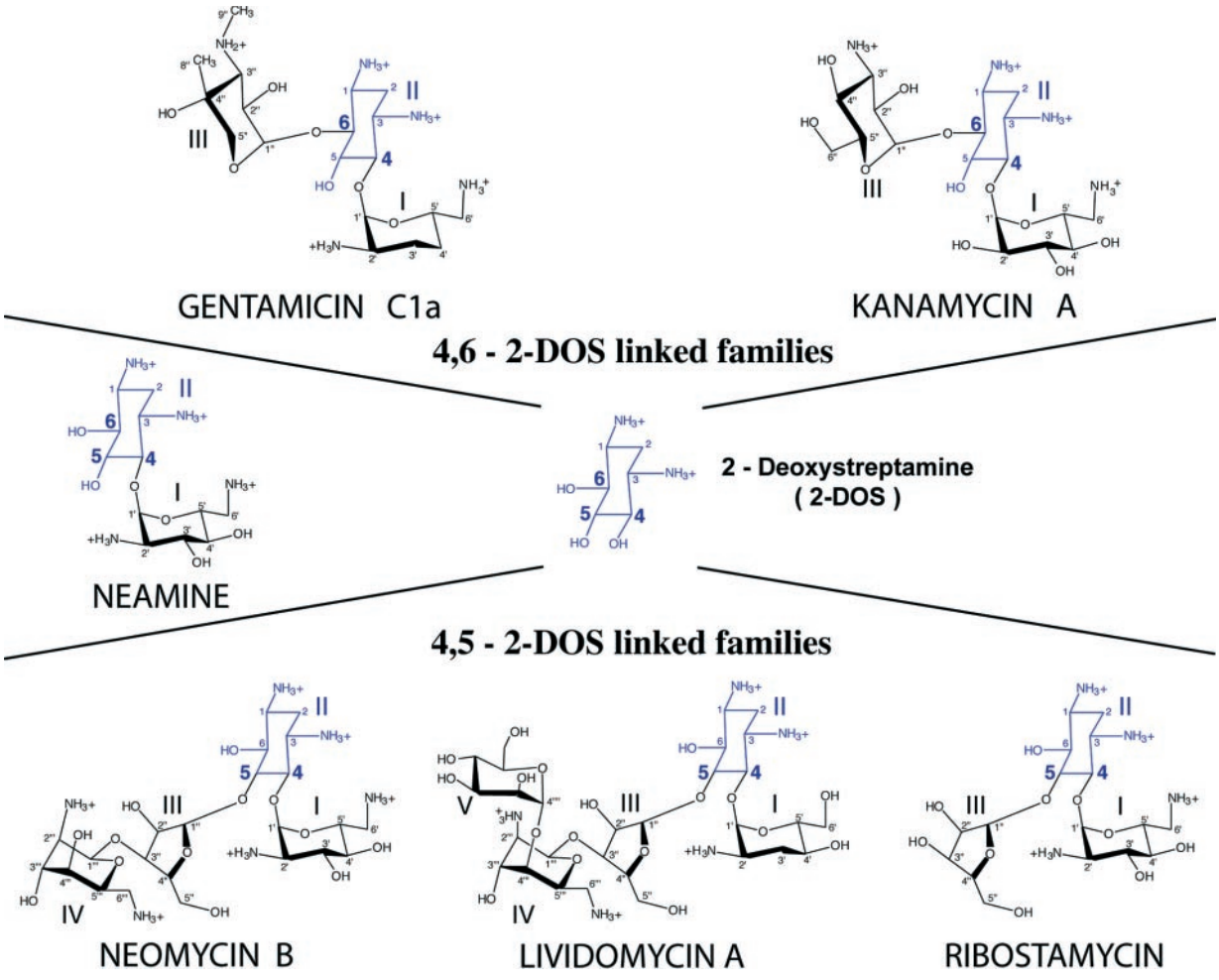

Figure 1. Chemical structures of the three aminoglycoside subclasses studied in this work. The common 2-deoxystreptamine ring is coloured in blue and the substituted positions are numbered in bold.

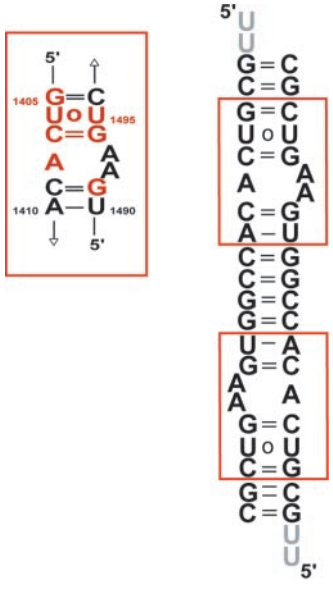

Figure 2. Left: secondary structure of the minimal A site. The standard *E.coli* numbering is used. Right: secondary structure of the crystallized RNA helix. The two A sites are boxed and the 5′-dangling UU, usually not observed in the density maps, are shaded.

geneticin characterized the binding mode of aminoglycosides at high resolution. The puckered sugar ring I is inserted into the A site helix by stacking against a guanine residue (G1491) and by forming a pseudo pair with two H-bonds to the Watson–Crick sites of an universally conserved adenine (A1408). This particular interaction helps to maintain adenines A1492 and A1493 in the bulged-out conformation which allows those two adenines to make A-minor contacts with two Watson–Crick base pairs. In the 30S particle, the two contacted Watson–Crick base pairs belong to the first two pairs of the codon-anticodon minihelix (4–6). In the co-crystal structures, the two contacted Watson–Crick base pairs belong to a neighbouring complex, mimicking the situation occurring in the 30S particle (8,11). This locked conformation of the bulging A1492 and A1493 in the docked complex forms the molecular basis for the aminoglycoside induced misreading (5,12). The conserved 2-deoxystreptamine ring (ring II) forms similar H-bonds in the three complexes and its binding is made possible by the adaptability created by the universally conserved U1406·U1495 pair. The additional rings contact different nucleotides of the A site, depending on the substitution type of ring II. Thus, overall tight packing of atoms in direct van der Waals contact is central and a prerequisite to specific recognition. About one third of the total RNA-aminoglycoside

contacts were shown to be mediated by water molecules (11). Water molecules participate in the assembly by linking hydrophilic groups that belong to both components. The hydration shells around nucleic acid base pairs tend to be conserved and maintained regardless of the environment (13,14).

Here, we present six crystal structures of complexes between A site oligonucleotides and aminoglycoside antibiotics containing between two and five aminosugar rings: neamine (2.5 Å), ribostamycin (2.2 Å), kanamycin A (3.0 Å), gentamicin C1A (2.8 Å), neomycin B (2.4 Å) and lividomycin A (2.2 Å) (Supplementary Table 1). Those crystal structures fully confirm the conservation of contacts between aminoglycosides and A site nucleotides despite the great molecular variety: eight direct contacts between the neamine rings and the A site nucleotides are present in every single crystal structure. In addition and following the molecular diversity, the complexes display various additional contacts, either direct or water-mediated to the neamine moiety as well as to the additional rings. The crystal structures also show that the occupancy at the binding site can be variable. Thus, in the neamine crystal structure, one of the two A sites is empty; in the kanamycin complex, one A site contains two bound antibiotics; and, in the ribostamycin complex, both A sites contain two bound antibiotics. Overall, the stoichiometry of aminoglycoside binding is observed to vary between zero and two per A site, an important fact which needs to be incorporated in the appreciation of the measured binding constants on model oligonucleotide systems and in their comparisons with structural data.

MATERIALS AND METHODS

Crystallization procedures are essentially the same as published previously (8–10). Two RNA constructs were used for crystallization trials: 5′-CGCGUCACACCGGUGAAGUCGC-3′ and 5′-UUGCGUCACACCGGUGAAGUCGC-3′. These were purchased from Dharmacon Research, Inc (Boulder, CO) and purified by denaturing gel electrophoresis [20%(w/v) acrylamide/bisacrylmamide (19:1), 8 M urea] using TBE buffer [9 mM Tris-borate (pH 8.3) and 0.2 mM EDTA] at 50–55°C. The appropriate band was excised, eluted into 300 mM Sodium Acetate pH 5.2 and recovered by precipitation with iso-propanol. The RNA was exchanged and concentrated to 2.0 mM into 100 mM Sodium Cacodylate pH 6.4, 50 mM Sodium Chloride, 5.125 mM Magnesium Sulphate and 0.125 mM EDTA. Before crystallization the RNA was annealed by heating at 90°C for 2 min and then slowly cooled to 37°C. Antibiotics were purchased from Sigma, and made up to 4 mM in 200 mM Sodium Cacodylate pH 6.4 and 300 mM Potassium Chloride. Equal volumes of RNA and antibiotic solution were combined and incubated at 37°C for 10 min before crystallization. Crystallization was performed by the hanging drop method as follows, 1 µl of RNA/antibiotic solution was combined with 1 µl of crystallization solution (1–5% MPD and 1–5% glycerol) and equilibrated over a 50% MPD (Fluka) reservoir.

The best crystals were recovered and vitrified in liquid ethane (110 K) or nitrogen (77 K) after soaking briefly in 12.5 mM Sodium Chloride, 125 mM Sodium Cacodylate pH 6.4, 150 mM Potassium Chloride, 2 mM Antibiotic and 40% MPD.

Data collection was performed on the Structural Biology Beamline ID29 at the European Synchrotron Radiation Facility (ESRF; Grenoble, France). Data were processed with the HKL2000 suite (15) and a correct solution was found for each structure by the molecular replacement program Molrep (16) using the coordinates of the RNA from PDB code 1J7T (paromomycin). Refinement was done using CNS version 1.1 (17). The parameter and topology files for the antibiotic molecules were obtained on the Hetero-compound Information Centre—Uppsala server (18) (University of Uppsala, Sweden). The data pertaining to data collection and refinement are given in Supplementary Table 1. Each crystallized duplex contains two identical but independent A sites. In all complexes, one of the two A sites is always better defined structurally (lower temperature factors, more identified solvent peaks). The structure of the complex with neamine has been refined at 2.8 Å as well as in the presence of modified neamine molecules (J.B. Murray, S.O. Meroueh, R.J.M. Russell, G. Lentzen, J. Haddad, S. Mobashery, submitted) (19). Here we extended the refinement to 2.5 Å. In all figures below, only the better defined A site is used for representation. All figures were drawn using The PyMOL Molecular Graphics system (2002) DeLano Scientific, San Carlos, CA (http://www.pymol.org).

RESULTS

First, the complexes that display the same main characteristics as the previously published ones will be described. That section will be followed by the complexes displaying non-specifically bound antibiotics. The crystal structure of the complex between neamine and the RNA oligonucleotide is discussed separately owing to its peculiarities. Finally, there is a description of the crystal packing contacts and of their importance.

Standard complexes

The complexes are described with increasing number of rings additional to the neamine moiety. Supplementary Tables 2A–C contains a list of hydrogen bonding contacts, direct or water-mediated, between the rings of the aminoglycosides and the RNA duplex. In Supplementary Table 3, the root-mean-square-deviations (RMSD) of the RNA duplexes in all the complexes are shown. When considering only the minimal A site nucleotides, the RMSD values are between 0.4 and 0.9 Å, independently of the nature of the 4,5 or 4,6 linkage. When considering all atoms of the RNA duplexes, the values are slightly higher and tend to be a little higher when comparing 4,5 and 4,6 substituted aminoglycosides (but still less than 1.2 Å). Such comparisons cannot include the complex with neamine (see below). The comparisons are made with respect to the paromomycin complex (8) which is the only A site bound aminoglycoside solved also within the context of the 30S particles (7). We showed before (8) that the RMSDs between the complexed oligonucleotide crystals and the complexed 30S particles are less than 1 Å. Comparisons between the RNA alone structures of the present complexes and the A site RNA in the paromomycin bound 30S particles (7) are also around 1 Å.

Gentamicin C1A

The gentamicin C1A is a 4,6 aminoglycoside very closely related to geneticin (also known as gentamicin G or G418). The differences are in ring I where the important 6′ substituent is an ammonium group and carbons 3′ and 4′ are deoxy. Six of the eight invariant intermolecular contacts between rings I and II are present, the two missing ones being those involving the hydroxyl groups at the 3′ and 4′ positions. Of those six, four are absent in the NMR structure (distances above 3.5 Å) (20). Such differences have been discussed previously (8,21). Four contacts are common in both gentamicin C1A and geneticin crystals (10) (Figure 3 and Supplementary Tables 2A–C). The U1495·U1406 base pair is bifurcated with a H-bond between O4″ and O2P(U1406) as in geneticin. The intramolecular H-bond between N2′ and O5 linking rings II and I is water-mediated in geneticin and direct in gentamicin, while the other intramolecular H-bond, between O5 and O5″ linking rings I and III are direct in both. The RMSD between the X-ray and NMR structure (20) is 2.3 Å while the RMSD between the present X-ray complex and the paromomycin bound to the 30S particle (7) is 1.0 Å.

Neomycin B

Neomycin B is a 4,5 aminoglycoside which differs from paromomycin by the presence of an ammonium group instead of a hydroxyl group at position 6′. It thus carries six positive charges, being the aminoglycoside with the highest charge. The number of aminoglycoside/RNA contacts is about the same in paromomycin and neomycin, respectively, (23,24) with 15 common factors (Figure 4 and Supplementary Tables 2A–C). Again, the U1495·U1406 base pair is bifurcated with a water mediated contact between O4(U1406) and O6 of ring II instead of a direct H-bond as in gentamicin and geneticin.

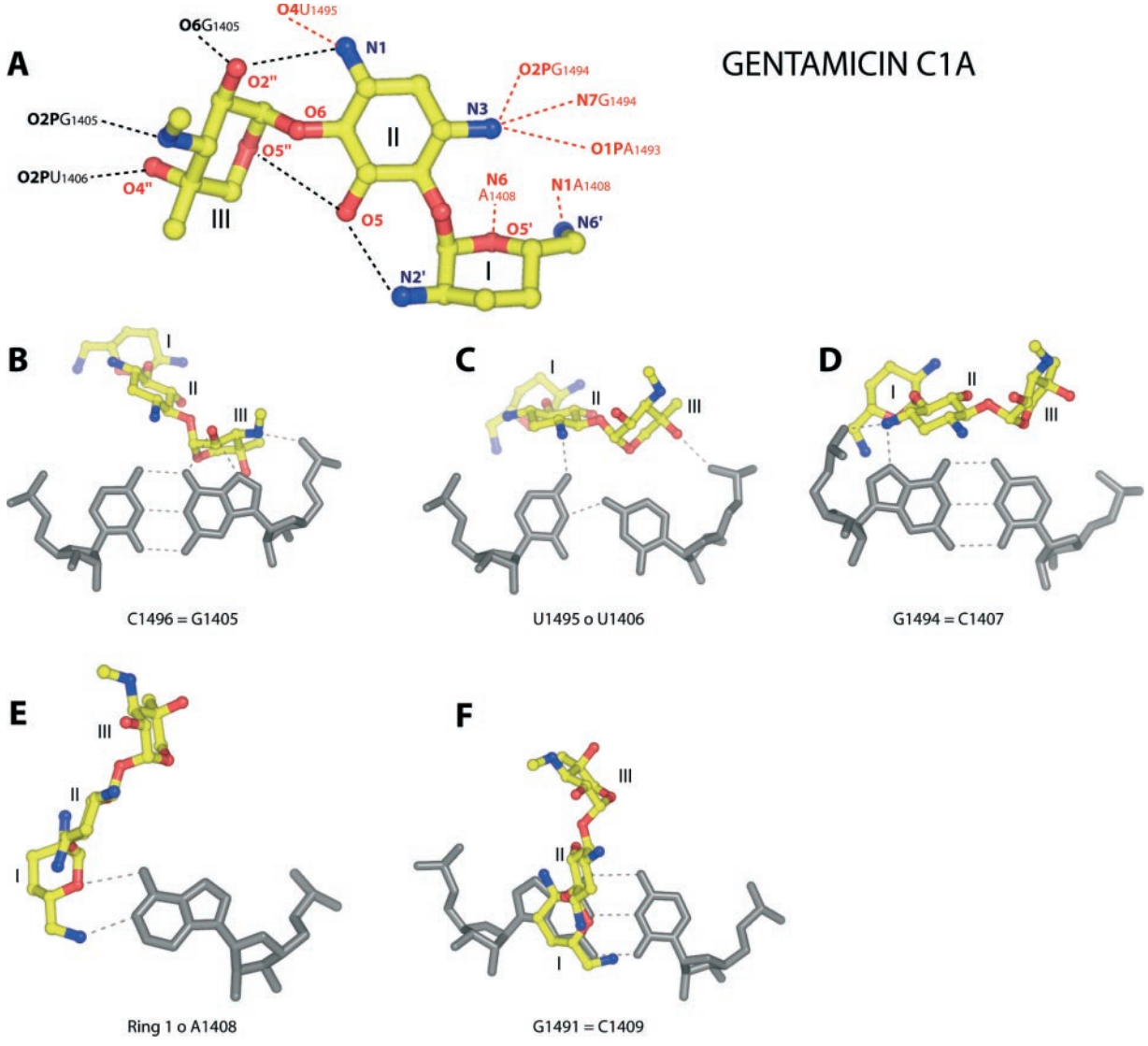

Figure 3. Description and analysis of the contacts between gentamicin C1A and the RNA fragment. **(A)** Structure adopted by the gentamicin C1A molecule inside the A site of the duplex. Ring numbers (I–III) and atom names are specified. The *E.coli* numbering is used for the RNA atoms, and 'W' stands for water molecule. Hydrogen bonds are shown as dashed lines. Conserved contacts between gentamicin C1A and the minimal A site are shown in red. **(B–F)** Atomic details of the contacts involving each base pair of the minimal A site interacting with gentamicin C1A.

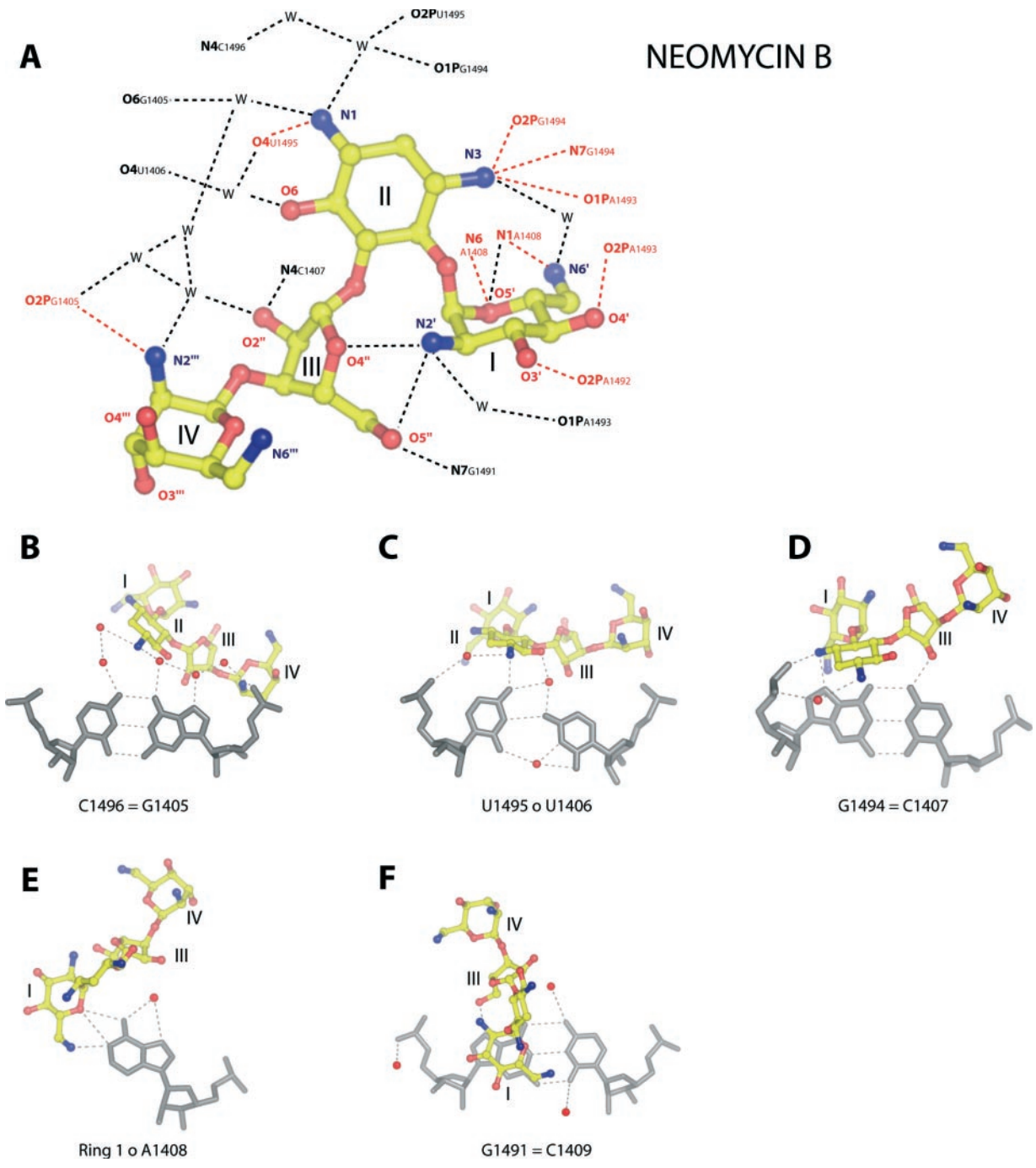

Figure 4. Description and analysis of the contacts between neomycin B and the RNA fragment. **(A)** Structure adopted by the neomycin B molecule inside the A site of the duplex. Ring numbers (I–IV) and atom names are specified. The *E.coli* numbering is used for the RNA atoms, and 'W' stands for water molecule. Hydrogen bonds are shown as dashed lines. Conserved contacts between neomycin B and the minimal A site are shown in red. **(B–F)** Atomic details of the contacts involving each base pair of the minimal A site interacting with neomycin B.

The two intramolecular H-bonds linking N2′ of ring I to O4″ and O5″ of ring II are identical.

Lividomycin A

Lividomycin A is also a 4,5 aminoglycoside but with five rings, the most substituted compound we have analysed. Position 6′ contains a hydroxyl group with a deoxy at position 3′. The last ring does not carry any positive charge and, thus, the overall charge is +5 like gentamicin. The resolution is among the highest of the crystals analysed (2.2 Å). Not surprisingly, the number of RNA/aminoglycoside contacts is high, 31, but with only 9 or 11 common between lividomycin and paromomycin or neomycin, respectively. Some of the differences can be ascribed to a conformational change of the phosphate of A1493 leading to an alternative hydration network between the neamine part and the RNA (Figure 5). In the complex of geneticin, this alternative conformer of A1493 was observed in

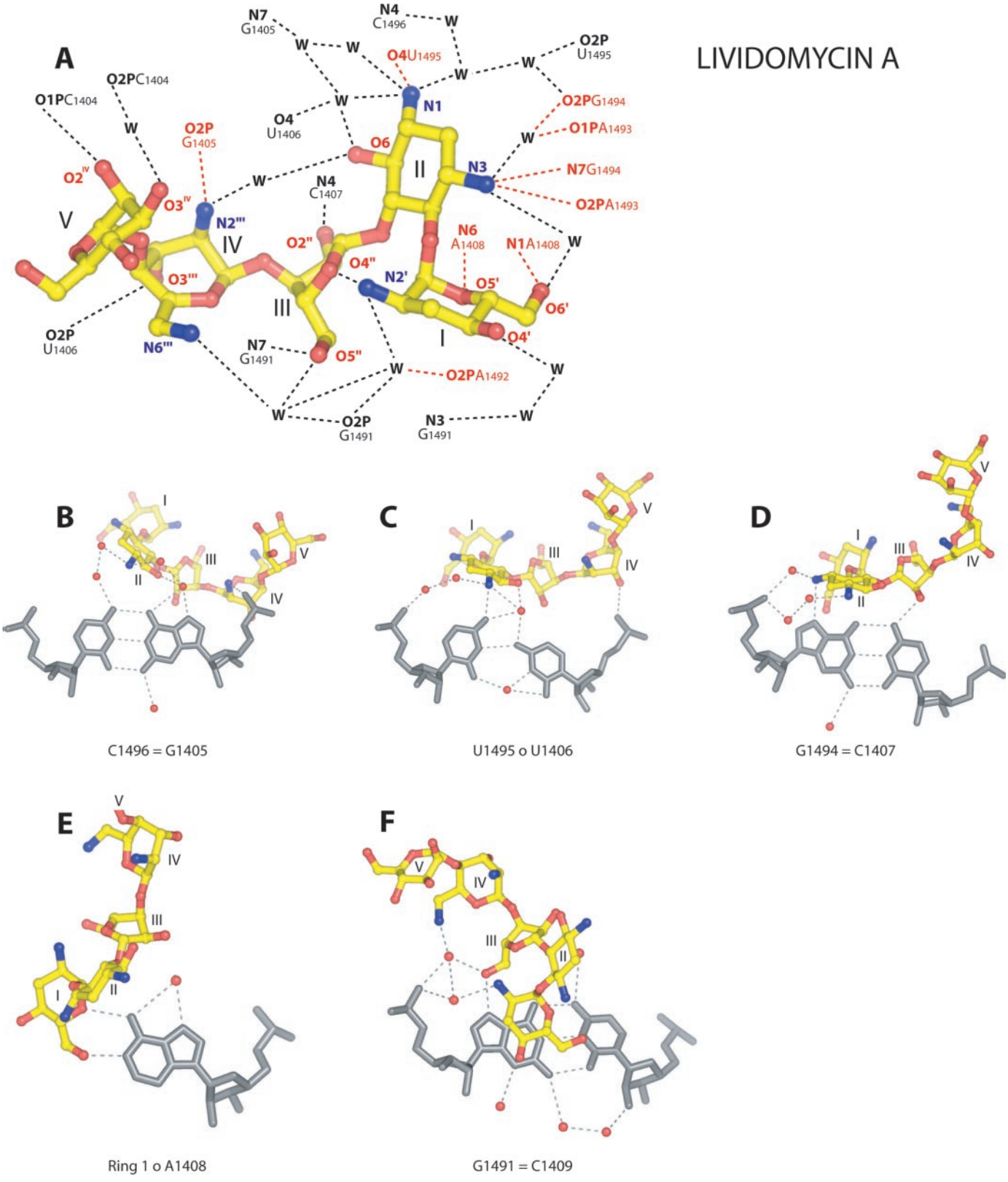

Figure 5. Description and analysis of the contacts between lividomycin A and the RNA fragment. **(A)** Structure adopted by the lividomycin A molecule inside the A site of the duplex. Ring numbers (I–V) and atom names are specified. The *E.coli* numbering is used for the RNA atoms, and 'W' stands for water molecule. Hydrogen bonds are shown as dashed lines. Conserved contacts between lividomycin A and the minimal A site are shown in red. **(B–F)** Atomic details of the contacts involving each base pair of the minimal A site interacting with lividomycin A.

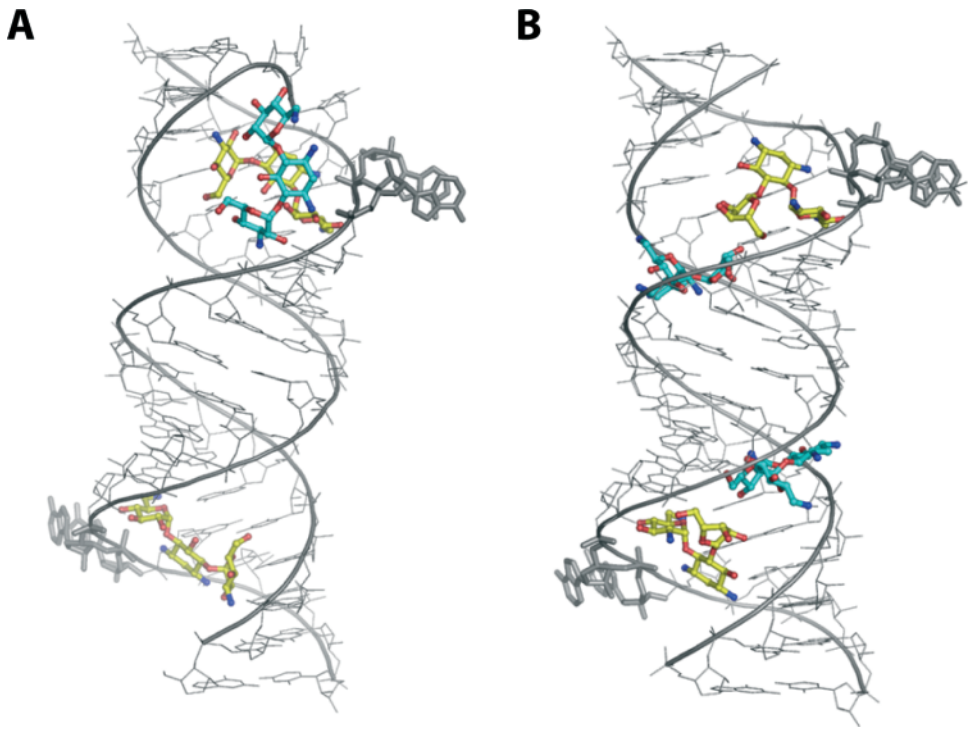

Figure 6. Specific and 'non-specific' binding modes of aminoglycosides. **(A)** Overall view of crystallized kanamycin A complex. **(B)** Overall view of crystallized ribostamycin complex. In both structures, the specifically bound antibiotics are coloured in yellow ball and sticks and the 'non-specifically' bound antibiotics are coloured in cyan ball and sticks.

equilibrium with the regularly seen conformer. Again, the U1495·U1406 base pair is bifurcated with two bound water molecules, one linking the RNA to the aminoglycoside and the other one bound to U1406. The hydroxyl groups of ring V contacts only single anionic phosphate oxygen atoms.

Complexes with both specific and non-specific binding

Two complexes displayed unexpected stoichiometries. In the crystal structure of the complex between kanamycin and the oligonucleotide, one A site contained a single antibiotic as usual but the second A site (with the lowest B-factors) presented two bound aminoglycosides, one in the standard binding mode and the second one in a new binding mode (Figure 6A). Further, in the complex between ribostamycin and the oligonucleotides, both A sites contained two bound aminoglycosides, one in the standard binding mode and the other one still in another binding mode (Figure 6B). We refer to these additional binding modes as 'unspecific' binding modes not only order to distinguish the binding modes but also because of the diversity in the binding modes of the 'unspecific' ones.

Kanamycin A

Kanamycin A is a 4,6 aminoglycoside with two changes compared to tobramycin: there is a hydroxyl group at position 3′ and position 2′ contains a hydroxyl group instead of an ammonium group as in tobramycin. Thus, overall, kanamycin carries four positive charges instead of five charges. Tobramycin and kanamycin present, respectively, 21 and 20 RNA/aminoglycoside contacts. Of those, eight contacts belong to the common and usual eight invariant contacts (Figure 7). In the best defined A site, there is a second kanamycin molecule straddling the entrance of the deep/major groove (Figure 7G). The conformations of the specifically and unspecifically bound kanamycin molecules are almost identical (RMSD of 0.5 Å with the RMSD between the two specifically bound kanamycin equal to 0.2 Å). The substituents on the rings make single H-bonds, six to water molecules and 5 to the RNA (Figure 7H). The two kanamycin molecules do not contact each other directly, but do interact via water molecules in an interesting fashion: the hydroxyl group O4″ of ring III binds a water molecule which links O2′ and O5 of rings I and II, respectively. Although dimeric aminoglycosides have been synthesized (22,23), it could be interesting attempting to synthesize dimeric molecules able to mimic the two crystallographic bound molecules observed in the present crystal structure.

Ribostamycin

Ribostamycin is a 4,5 aminoglycoside, equivalent to neomycin without ring IV. It, thus, carries only four positive charges. Compared to neomycin which makes 23 RNA/aminoglycoside contacts, the specifically bound ribostamycin makes 21 but, among those, 13 are common to both complexes (Figure 8 and Supplementary Tables 2A–C): the hydroxyl O5″ of ring III, instead of H-bonding to N7(G1491), H-bonds to O6(G1491). As discussed above, in both A sites, two ribostamycin molecules are bound (Figure 8G). The conformers of the ribostamycin molecules, the specifically and the unspecifically bound ones, are almost identical (RMSD specific-unspecific = 0.8 Å, RMSD specific-specific = 0.4 Å). In contrast to the situation observed in the kanamycin complex, the ribostamycin molecules face each other with their rings III but

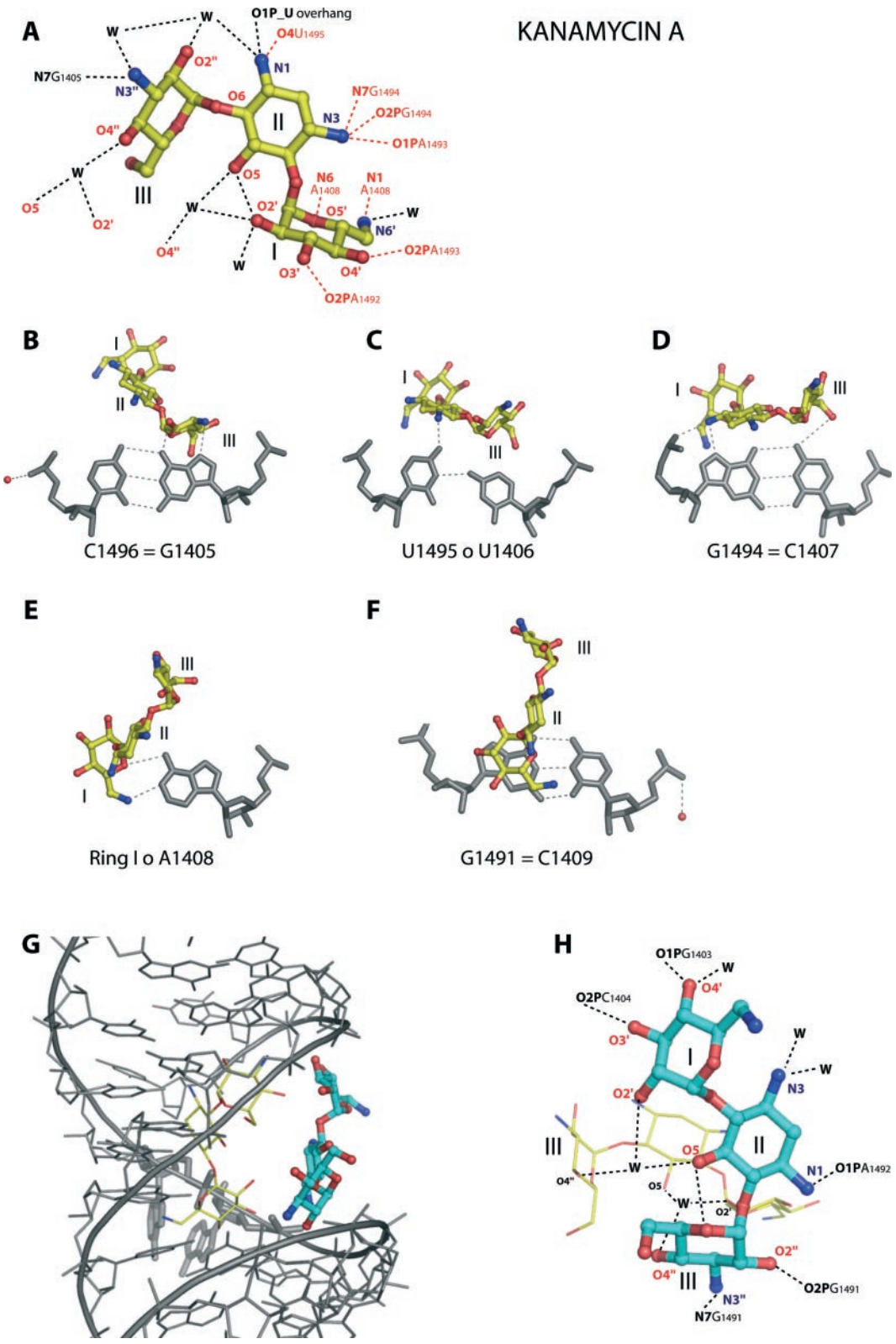

Figure 7. Specific binding of kanamycin A. **(A)** Structure adopted by the specific kanamycin molecule coloured in yellow ball and sticks inside the A site of the duplex. Ring numbers (I–III) and atom names are specified. The *E.coli* numbering is used for the RNA atoms, and 'W' stands for water molecule. Hydrogen bonds are shown in dashed lines. Conserved contacts between specific kanamycin and the minimal A site are shown in red. **(B–F)** Atomic details of the contacts involving each base pair of the minimal A site interacting with the two kanamycin molecules. **(G)** Position of the non-specifically bound kanamycin (coloured in cyan ball and sticks) at the entrance of the deep/major groove of the A site duplex. The specific molecule of kanamycin is coloured in yellow lines. **(H)** Contacts made by the 'non-specific' kanamycin, Ring numbers (I–III) and atom names are specified. The *E.coli* numbering is used for the RNA atoms, and 'W' stands for water molecule. Hydrogen bonds are shown as dashed lines.

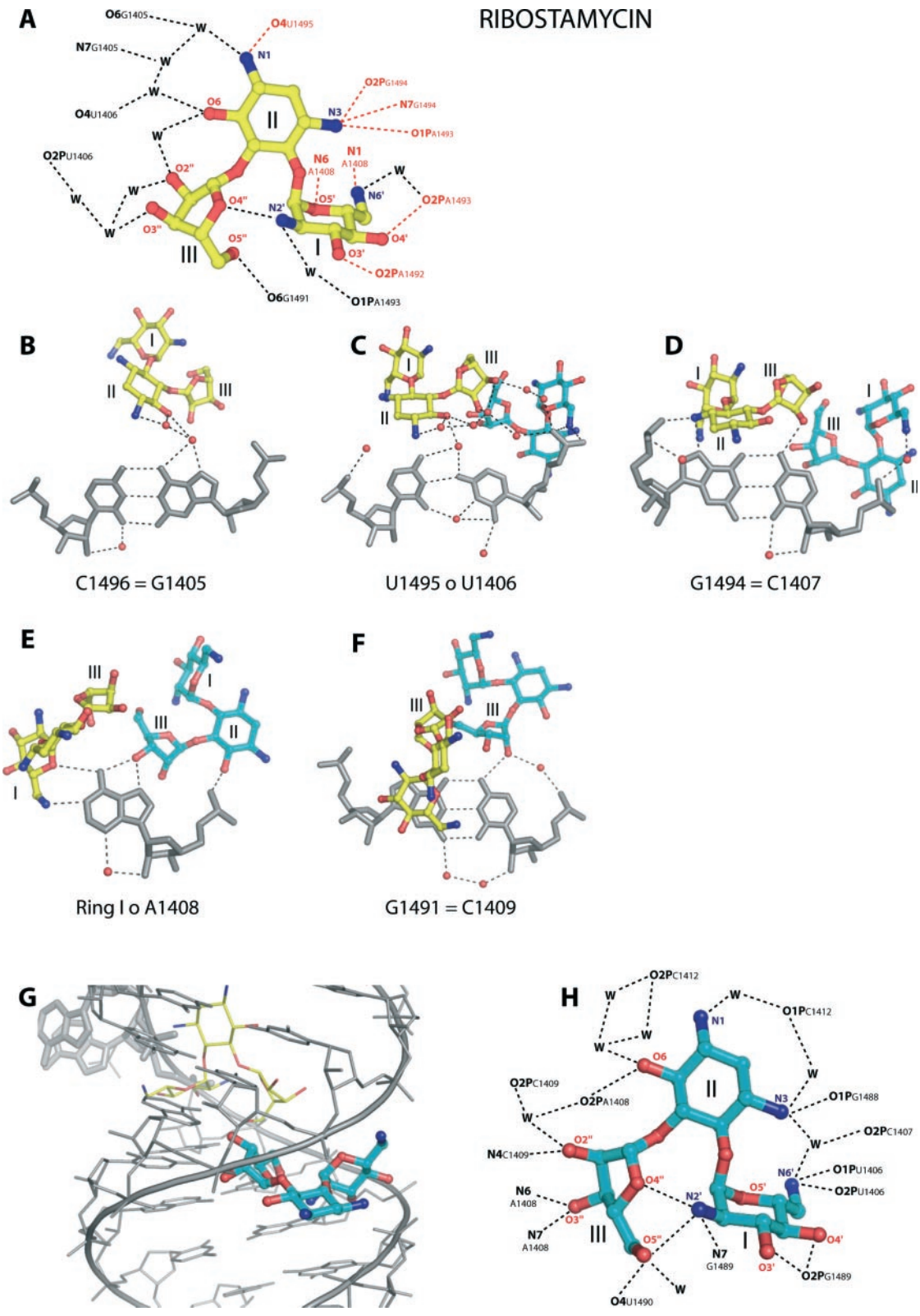

Figure 8. Specific and 'non-specific' binding of ribostamycin. **(A)** Structure adopted by the specific ribostamycin molecule coloured in yellow ball and sticks inside the A site of the duplex. Ring numbers (I–III) and atom names are specified. The *E.coli* numbering is used for the RNA atoms, and 'W' stands for water molecule. Hydrogen bonds are shown as dashed lines. **(B–C)** Conserved contacts between specific kanamycin and the first two base pairs of the minimal A site are shown in red. **(D–F)** Atomic details of the contacts involving the base pairs of the minimal A site interacting with the two ribostamycin molecules. **(G)** Position of ribostamycin non-specifically bound (coloured in cyan ball and sticks) at the entrance of the deep/major groove of the duplex. The specifically bound molecule of ribostamycin is coloured in yellow lines. **(H)** Contacts made by the 'non-specific' ribostamycin, Ring numbers (I–III) and atom names are specified. The *E.coli* numbering is used for the RNA atoms, and 'W' stands for water molecule. Hydrogen bonds are shown as dashed lines.

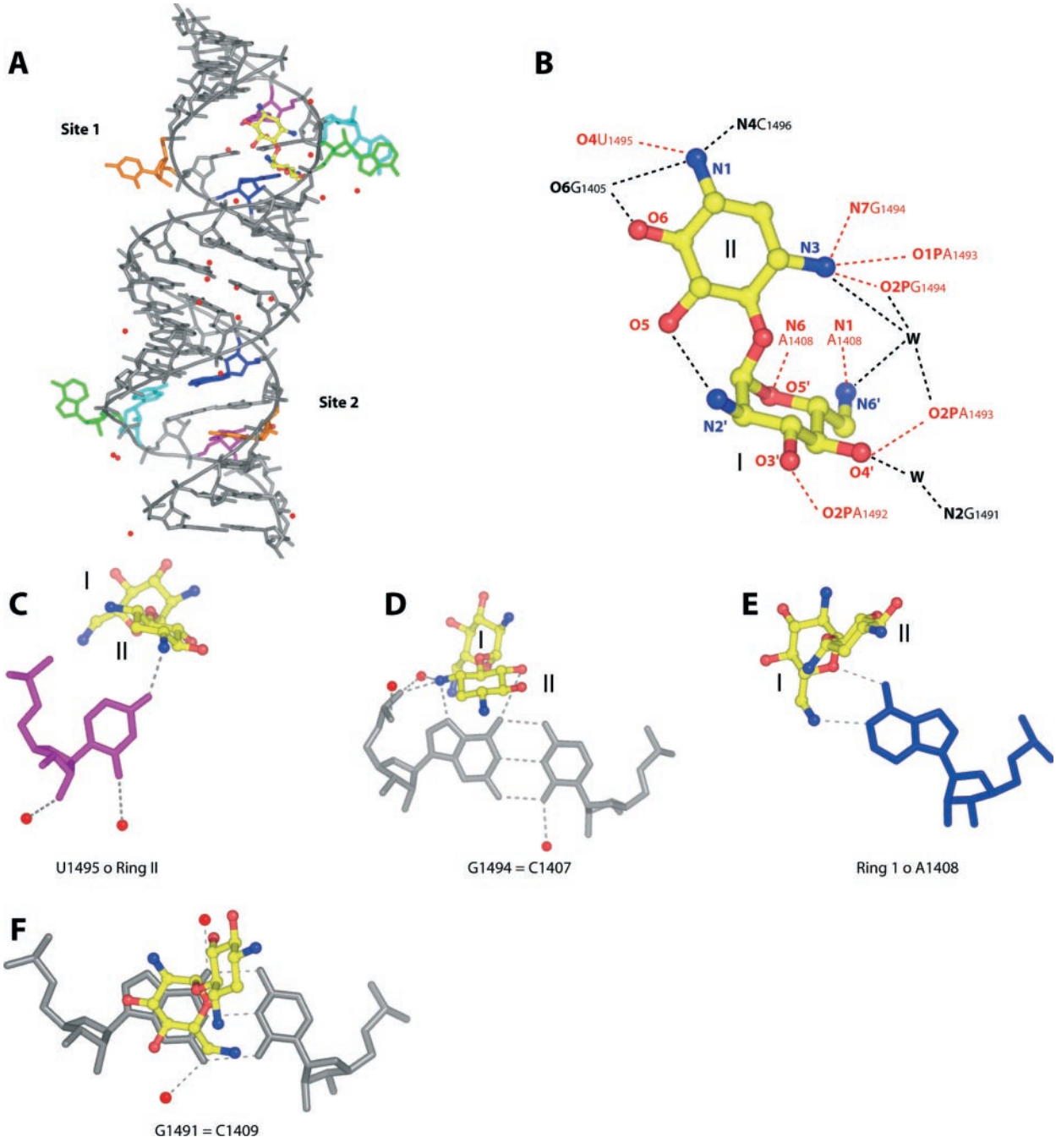

Figure 9. Description and analysis of the contacts between **neamine** and the RNA fragment. **(A)** Overall view of the crystallized complex. Site 1 contains one neamine in yellow. In both sites, A1408 are coloured in dark blue, A1492 in green, A1493 in cyan, U1406 in orange (which makes intermolecular contacts with C1405-G1491) and U1495 in magenta [which makes contacts with A1492 of site 2 of a symmetric molecule, see (D)]. **(B)** Ring numbers (I and II) and atom names are specified. The *E.coli* numbering is used for the RNA atoms, and 'W' stands for water molecule. Hydrogen bonds are shown as dashed lines. Conserved contacts between neamine and the minimal A Site are shown in red. **(C–F)** Atomic details of the contacts involving each base pair interacting with neamine in site 1.

do not contact each other, even via water molecules (although this cannot be formally excluded owing to the moderate resolution). On the contrary, the two ribostamycin molecules bind to common nucleotides of the A site: the O3″ and O2″ of ring III interacts with N6 and N7 of A1408 as well as with N4 and O2P of C1409, respectively, (Figure 8E, F and H). Rings I and II of the unspecifically bound ribostamycin interacts with nucleotides 'below' the conserved region of the A site (1412, 1488, 1489) (Figure 8H).

The complex with neamine: variable occupancy

The crystal structure of the complex between neamine and the oligonucleotides is the most peculiar one. All the standard direct H-bonds between the neamine rings and the RNA are present with the two A1492 and A1493 bulging out as in all other complexes (Figure 9). However, U1406 does not form a base pair with U1495 but, instead, bulges out of the duplex. The place normally occupied by U1406 is filled in by an

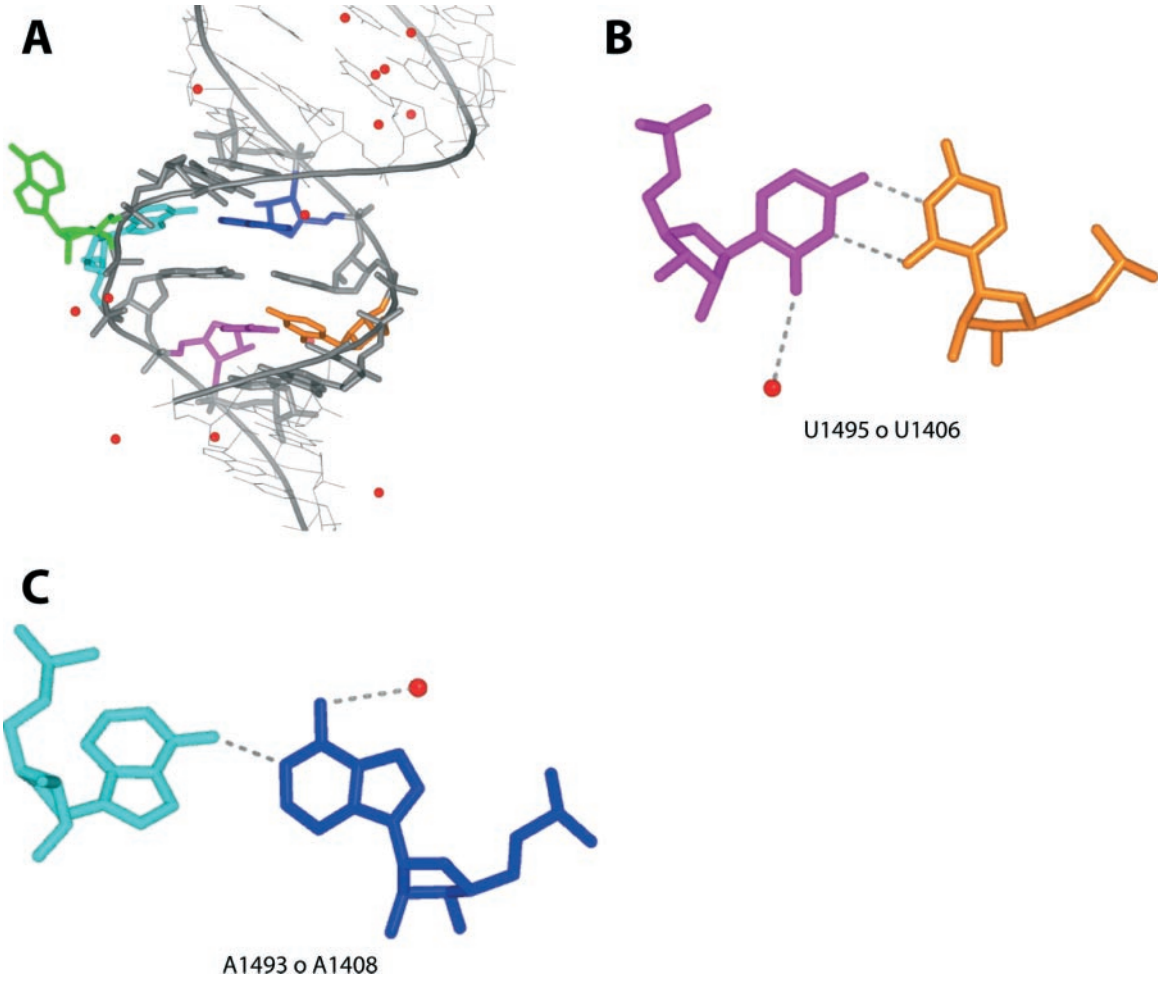

Figure 10. Description of the empty A site of the crystallized neamine complex. **(A)** Overall view of site 2. A1408 is coloured in dark blue, A1492 in green, A1493 in cyan, U1406 in orange and U1495 in magenta. (**B** and **C**) Atomic details of the base pair interactions into the empty minimal A site. Hydrogen bonds are shown as dashed lines.

A1492 from a neighbouring molecule, forming a *cis* Watson–Crick/Hoogsteen pair (with the adenine in the *syn* conformation). The second site is void of antibiotic and adenine A1408 forms a single H-bond pair with A1493 in the *syn* conformation (Figure 10C), while the U1406·U1495 base pair is fully symmetric. Only A1492 bulges out (and H-bonds to a neighbouring molecule U1495, as just described). Such a conformation with the bulging U1406 is compatible with the conformation of the A site in the 30S ribosomal particle complexed to tRNA and mRNA (6) (Supplementary Figure 1). An isomorphous structure was obtained for complexes with neamine at a lower resolution as well as with modified neamine molecules (J.B. Murray, S.O. Meroueh, R.J.M. Russell, G. Lentzen, J. Haddad, S. Mobashery, submitted) (19). Interestingly, in crystals of oligonucleotides containing a single A site (24), an equilibrium between the flipped out conformation of both A1492 and A1493 and a conformation with only A1493 flipped out was observed. The latter conformation is different from the one observed in the free A site of the neamine complex, since a *cis* Watson–Crick between A1408 and A1492 was observed (24). Thus, the free A site exists in multiple and alternative conformations in contrast to the aminoglycoside complexed A site, as observed previously (7,24).

Crystal packing: Adenines 1492 and 1493 bulge out of the A site helix to form A-minor contacts with the first two base pairs of the codon–anticodon

The previous structures of the minimal A site RNA complexed to various aminoglycosides display crystal packings in which the main intermolecular contacts occur between the bulging adenines (A1492 and A1493) and the shallow/minor groove of a neighbouring helix (11). The two adenines interact with the 3′ ends of two adjacent helical Watson–Crick base pairs such that the first adenine (A1492) interacts in an antiparallel fashion with one base of the Watson–Crick pair and the second adenine (A1493) interacts in a parallel fashion with one base of the next Watson–Crick pair. Such contacts have been called A-minor motifs (25). The type I and type II names correspond to the *trans* sugar-edge/sugar-edge or *cis* sugar-edge/sugar-edge base pairs (26) (Figure 11). Two important points can be raised: (i) A1493 interacts with both strands of the receptor helix, whereas A1492 interacts only with one strand; (ii) A1493 forms more H-bonds than A1492. In all crystal structures of RNA/Aminoglycoside complexes (the previous ones (8–10) and those reported here), for at least one of the two sites, the two bulging adenines form ideal A-minor motifs with a neighbouring molecule (Supplementary Figure 3 shows a

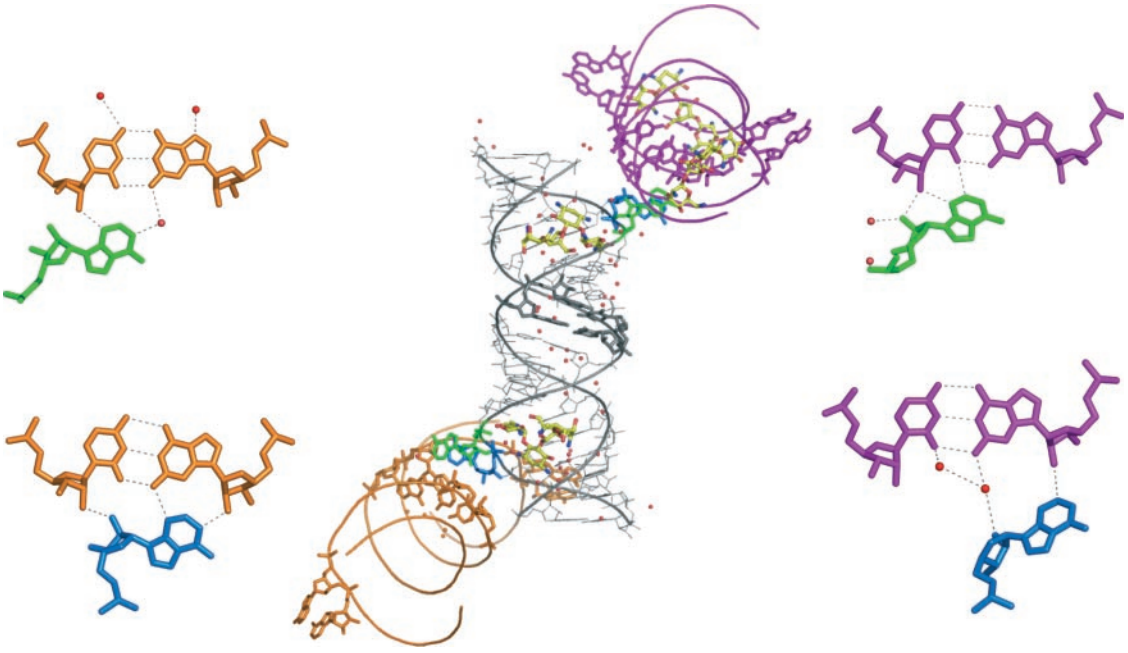

Figure 11. Three-dimensional structure of the packing interactions observed in the neomycin B crystal at the central Watson–Crick domain of the duplex. This view shows a central duplex interacting with two symmetry-related duplexes via the bulged adenines. In both A sites, A1492 are coloured in green, A1493 in cyan and red spheres indicate water molecules. Close-up of the interactions between each adenine and its counterpart G = C pair (on the right magenta in site 1, top of central drawing and, on the left orange in site 2, bottom of the central drawing). The hydrogen bonds are represented by black dashed lines.

superimposition of all the structures). Although the packing is more complicated for the neamine complex, A1492 and A1493 of the bound site do form A-minor motifs with a neighbouring duplex (Supplementary Figure 2).

DISCUSSION

It has been shown that aminoglycosides disturb the fidelity of the tRNA selection step by stabilizing a conformation similar to that obtained for near-cognate complexes (4–6,12,27). In other words, aminoglycosides provoke a structural rearrangement of the decoding site from a state in which it accepts the tRNA to a conformation which is productive for peptide bond synthesis even in the absence of cognate mRNA/tRNA complexes (7). Crystallographic structures of various 30S ribosomal particles and the present minimal A site complexes bound to aminoglycosides (together with the previous ones) offer different snapshots that helped to visualize atomic details of the mechanism of action of aminoglycosides. During decoding, the A site changes its conformation from an 'off' conformation (with A1492 and A1493 folded into the shallow groove of the A site) to an 'on' conformation (with A1492 and A1493 fully bulged out from the A site) (4–7). The crystal structure of the neamine complex gives one possible view of the 'off' conformation with a single adenine bulging out and the other one paired within the A site. Recent elegant experiments (24) coupling X-ray crystallography and fluorescence of 2-amino purine substituted A1492 and A1493 fully confirm that interpretation. A different set of experiments (28), using equilibrium dialysis of 2′-O-methyl oligoribonucleotides devised for binding to the A site of 30S particles, came to a similar conclusion. The observed conformational change is necessary to allow A1492 and A1493 to interact specifically with the first two of the three base pairs formed by the cognate codon–anticodon interaction. The crystal packing observed in all complexes display the same types of contacts between the bulging adenines and Watson–Crick base pairs of a neighbouring duplex. This observation was used to screen crystallographically compounds for specific binding to the A site. In this way, modified aminoglycosides with activity against resistant bacteria could be crystallized and their structures solved (29). The work on modified aminoglycosides (29), as well as the data on the minimal inhibitory concentrations of natural aminoglycosides (30,31) confirm *a posteriori* the biological relevance of the present crystal complexes and their validity as models for the complexes between the 30S particles and aminoglycosides (7). Our present observations further support the view that the A site exists in a dynamic equilibrium between conformations in which A1492 and A1493 are fully bulged out and those in which only one base is bulging out with the other one tucked inside the A site.

CONCLUSIONS

In the last five years, crystal structures of complexes between various antibiotics and ribosomal particles or oligonucleotides containing rRNA fragments [for a recent review, see (32)] have offered us detailed views of the molecular recognition between RNA targets and drugs. The comparative structural analysis of this work leads to the following main conclusions: (i) up to eight conserved contacts are observed in the complexes; (ii) the conformations of the natural aminoglycosides are always very similar; (iii) the aminoglycosides with the

least amount of charges and/or of rings tend to bind A site RNAs unspecifically in addition to specific binding.

(i) The conservation of contacts between the nine different aminoglycosides, either 4,5 or 4,6 substituted, and the ribosomal A site is clearly established. Despite the molecular diversity in the antibiotics, key characteristic and common interactions between aminoglycosides and the A site are conserved: (a) the intercalation of ring I; (b) the pseudo base pair between A1408 and ring I; (c) the contacts between the nitrogens of the 2-DOS, N1 to O4(U1495), N3 to N7(G1494), O2P(G1494), O1P(A1493). Besides these six H-bonds, the contacts between the hydroxyl groups O3′ and O4′ of ring I to the phosphate groups of A1492 and A1493 occur depending on the presence of the hydroxyl groups. It is striking to notice that the recent crystal structure of the complex between the unrelated aminoglycoside apramycin and the same oligonucleotide displayed, in addition to new contacts, the same invariant contacts between the 2-DOS as well as between the bicyclic ring II and the same nucleotides A1408, G1494 and U1495 (33).

(ii) Variable contacts between the additional rings and the RNA are formed depending on the number of the rings, several of which are mediated by water molecules. The overall conformations of the aminoglycosides are always very similar; even when the aminoglycosides are bound unspecifically at the edges of the A site (RMSD values below 0.5 Å). This result is in stark contrast to the recent crystal structures of complexes between the same oligonucleotide and aminoglycosides modified at the 2″ position by chains of various length (29) where a large movement of rings III and IV could be observed. Thus, natural aminoglycosides maintain the same exact conformation in different binding modes in crystals, while they are flexible enough to form very different conformations in other complexes with non-natural substitutions.

(iii) The least charged aminoglycosides among the nine structures (neamine, ribostamycin, geneticin and kanamycin which have all four positive charges instead of five or more for the other five aminoglycosides) display unusual behaviours. In the geneticin crystal structure (10), alternative conformations of the sugar-phosphate backbone were observed around 1492 and 1493. In the neamine complex, an empty A site could be observed. In the ribostamycin complex, each A site contained two bound antibiotics, while in the kanamycin complex, only one A site contains two bound antibiotics. The binding modes of the unspecifically bound aminoglycosides are not comparable between each other, possibly reflecting the fact that one is a 4,5 and the other a 4,6 aminoglycoside. In any case, the structures illustrate the difficulty of predicting the proper stoichiometry of such complexes between oppositely charged molecules, confirming recent data showing discrepancies between measurements of affinity constants and minimal inhibitory concentrations (30). It is interesting to remark that both ribostamycin and kanamycin A, which both present unspecific binding, present the largest dissociation constants in the family of aminoglycosides studied (34). Noticeable for drug design, the weakly charged aminoglycosides with the least number of rings display variable stoichiometries with unspecific binding. The number of rings together with the number of positive charges therefore contribute both to the formation of the specific and high affinity 1:1 complexes.

In conclusion, the present comparative analysis of various aminoglycosides bound to the same ribosomal site helped us to decipher the contribution of each functional group to the specificity of the RNA/aminoglycoside complex and to derive structurally-based rules for the mechanisms of binding and action of that important family of antibiotics. However, the analysis also revealed the difficulties and pitfalls in attempting to rationalize the wealth of available thermodynamic binding data on the basis of crystallographic data.

SUPPLEMENTARY DATA

Supplementary Data are available at NAR Online.

ACKNOWLEDGEMENTS

We gratefully thank the European Synchrotron Radiation Facility for provision of synchrotron radiation facilities. B.F. is supported by fellowships from Ribotargets Ltd (Vernalis Ltd) and the E.E.C. project 'Ribosomal Inhibitors' (QLRT-2001-000892) coordinated by Wolfgang Wintermeyer. E.W. wishes to thank the Institut universitaire de France for support over the last ten years. Funding to pay the Open Access publication charges for this article was provided by CNRS funds.

Conflict of interest statement. None declared.

REFERENCES

1. Davies,J., Gorini,L. and Davis,B.D. (1965) Misreading of RNA codewords induced by aminoglycoside antibiotics. *Mol. Pharmacol.*, **1**, 93–106.
2. Moazed,D. and Noller,H.F. (1987) Interaction of antibiotics with functional sites in 16S ribosomal RNA. *Nature*, **327**, 389–394.
3. Wright,G.D., Berghuis,A.M. and Mobashery,S. (1998) Aminoglycoside antibiotics, structures, functions, and resistance. In Rosen,B.P. and Mobashery,S. (eds), *Resolving the antibiotic paradox: progress in understanding drug resistance and development of new antibiotics*. Kluwer Academic/Plenum Publishers, NY, pp. 27–69.
4. Ogle,J.M., Murphy,F.V., Tarry,M.J. and Ramakrishnan,V. (2002) Selection of tRNA by the ribosome requires a transition from an open to a closed form. *Cell*, **111**, 721–732.
5. Ogle,J.M., Carter,A.P. and Ramakrishnan,V. (2003) Insights into the decoding mechanism from recent ribosome structures. *Trends Biochem. Sci.*, **28**, 259–266.
6. Ogle,J.M., Brodersen,D.E., Clemons,W.M.,Jr, Tarry,M.J., Carter,A.P. and Ramakrishnan,V. (2001) Recognition of cognate transfer RNA by the 30S ribosomal subunit. *Science*, **292**, 897–902.
7. Carter,A.P., Clemons,W.M., Brodersen,D.E., Morgan-Warren,R.J., Wimberly,B.T. and Ramakrishnan,V. (2000) Functional insights from the structure of the 30S ribosomal subunit and its interactions with antibiotics. *Nature*, **407**, 340–348.
8. Vicens,Q. and Westhof,E. (2001) Crystal structure of paromomycin docked into the eubacterial ribosomal decoding A site. *Structure*, **9**, 647–658.
9. Vicens,Q. and Westhof,E. (2002) Crystal structure of a complex between the aminoglycoside tobramycin and an oligonucléotide containing the ribosomal decoding A site. *Chem. Biol.*, **9**, 747–755.
10. Vicens,Q. and Westhof,E. (2003) Crystal structure of geneticin bound to a bacterial 16S ribosomal RNA A site oligonucleotide. *J. Mol. Biol.*, **326**, 1175–1188.

11. Vicens,Q. and Westhof,E. (2003) RNA as a drug target: the case of aminoglycosides. *Chembiochem.*, **4**, 1018–1023.
12. Pape,T., Wintermeyer,W. and Rodnina,M.V. (2000) Conformational switch in the decoding region of 16S rRNA during aminoacyl-tRNA selection on the ribosome. *Nature Struct. Biol.*, **7**, 104–107.
13. Auffinger,P. and Westhof,E. (2000) Water and ion binding around RNA and DNA (C,G) oligomers. *J. Mol. Biol.*, **300**, 1113–1131.
14. Auffinger,P. and Westhof,E. (2001) Water and ion binding around r(UpA)12 and d(TpA)12 oligomers–comparison with RNA and DNA (CpG)12 duplexes. *J. Mol. Biol.*, **305**, 1057–1072.
15. Otwinowski,Z. and Minor,W. (1996) In Carter,C.W.J. and Sweet,R.M. (eds), *Methods in Enzymology*. Processing of X-ray diffraction data collected in oscillation mode, Academic Press, Vol. 276, pp. 307–326.
16. Collaborative Computing Project Number 4. (1994) The CCP4 suite: programs for protein crystallography. *Acta. Crystallogr. D Biol. Crystallogr.*, **50**, 760–763.
17. Brunger,A.T., Adams,P.D., Clore,G.M., DeLano,W.L., Gros,P., Grosse-Kunstleve,R.W., Jiang,J.S., Kuszewski,J., Nilges,M., Pannu,N.S. *et al.* (1998) Crystallography & NMR system: a new software suite for macromolecular structure determination. *Acta. Crystallogr. D Biol. Crystallogr.*, **54**, 905–921.
18. Kleywegt,G.J. and Jones,T.A. (1998) Databases in protein crystallography. *Acta. Crystallogr. D Biol. Crystallogr.*, **54**, 1119–1131.
19. Russell,R.J., Murray,J.B., Lentzen,G., Haddad,J. and Mobashery,S. (2003) The complex of a designer antibiotic with a model aminoacyl site of the 30S ribosomal subunit revealed by X-ray crystallography. *J. Am. Chem. Soc.*, **125**, 3410–3411.
20. Yoshizawa,S., Fourmy,D. and Puglisi,J.D. (1998) Structural origins of gentamicin antibiotic action. *EMBO J.*, **17**, 6437–6448.
21. Lynch,S.R., Gonzalez,R.L. and Puglisi,J.D. (2003) Comparison of X-ray crystal structure of the 30S subunit-antibiotic complex with NMR structure of decoding site oligonucleotide-paromomycin complex. *Structure (Camb)*, **11**, 43–53.
22. Michael,K., Wang,H. and Tor,Y. (1999) Enhanced RNA binding of dimerized aminoglycosides. *Bioorg. Med. Chem.*, **7**, 1361–1371.
23. Agnelli,F., Sucheck,S.J., Marby,K.A., Rabuka,D., Yao,S.L., Sears,P.S., Liang,F.S. and Wong,C.H. (2004) Dimeric aminoglycosides as antibiotics. *Angew Chem. Int. Ed. Engl.*, **43**, 1562–1566.
24. Shandrick,S., Zhao,Q., Han,Q., Ayida,B.K., Takahashi,M., Winters,G.C., Simonsen,K.B., Vourloumis,D. and Hermann,T. (2004) Monitoring molecular recognition of the ribosomal decoding site. *Angew Chem. Int. Ed. Engl.*, **43**, 3177–3182.
25. Nissen,P., Ippolito,J.A., Ban,N., Moore,P.B. and Steitz,T.A. (2001) RNA tertiary interactions in the large ribosomal subunit: the A-minor motif. *Proc. Natl Acad. Sci. USA*, **98**, 4899–4903.
26. Leontis,N.B. and Westhof,E. (2001) Geometric nomenclature and classification of RNA base pairs. *RNA*, **7**, 499–512.
27. Pape,T., Wintermeyer,W. and Rodnina,M. (1999) Induced fit in initial selection and proofreading of aminoacyl-tRNA on the ribosome. *EMBO J.*, **18**, 3800–3807.
28. Abelian,A., Walsh,A.P., Lentzen,G., Aboul-Ela,F. and Gait,M.J. (2004) Targeting the A site RNA of the *Escherichia coli* ribosomal 30 S subunit by 2′-O-methyl oligoribonucleotides: a quantitative equilibrium dialysis binding assay and differential effects of aminoglycoside antibiotics. *Biochem. J.*, **383**, 201–208.
29. Francois,B., Szychowski,J., Adhikari,S.S., Pachamuthu,K., Swayze,E.E., Griffey,R.H., Migawa,M.T., Westhof,E. and Hanessian,S. (2004) Antibacterial aminoglycosides with a modified mode of binding to the ribosomal-RNA decoding site. *Angew Chem. Int. Ed. Engl.*, **43**, 6735–6738.
30. Pfister,P., Hobbie,S., Brull,C., Corti,N., Vasella,A., Westhof,E. and Bottger,E.C. (2005) Mutagenesis of 16S rRNA C1409-G1491 base-pair differentiates between 6′OH and 6′NH3+ aminoglycosides. *J. Mol. Biol.*, **346**, 467–475.
31. Pfister,P., Hobbie,S., Vicens,Q., Bottger,E.C. and Westhof,E. (2003) The molecular basis for A site mutations conferring aminoglycoside resistance: relationship between ribosomal susceptibility and X-ray crystal structures. *ChemBioChem.*, **4**, 1078–1088.
32. Hermann,T. (2005) Drugs targeting the ribosome. *Curr. Opin. Struct. Biol.*, **15**, 355–366.
33. Han,Q., Zhao,Q., Fish,S., Simonsen,K.B., Vourloumis,D., Froelich,J.M., Wall,D. and Hermann,T. (2005) Molecular recognition by glycoside pseudo base pairs and triples in an apramycin-RNA complex. *Angew Chem. Int. Ed. Engl.*, **44**, 2694–2700.
34. Wong,C.H., Hendrix,M., Priestley,E.S. and Greenberg,W.A. (1998) Specificity of aminoglycoside antibiotics for the A site of the decoding region of ribosomal RNA. *Chem. Biol.*, **5**, 397–406.